

# ESTIMATING THE AVERAGE SIZE OF FIBER/MATRIX INTERFACE CRACKS IN UD AND CROSS-PLY LAMINATES

L. Di Stasio<sup>1,2</sup>, J. Varna<sup>1</sup>, Z. Ayadi<sup>2</sup>

<sup>1</sup> Division of Materials Science, Luleå University of Technology, Luleå, Sweden

<sup>2</sup>EEIGM & IJL, Université de Lorraine, Nancy, France

7<sup>th</sup> ECCOMAS Thematic Conference on the Mechanical Response of Composites  
Girona (ES) - September 18-20, 2019



## Outline

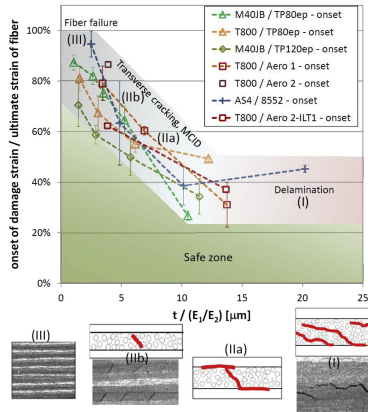
- ➔ Initiation of Transverse Cracks in Thin-plies
- ➔ Modeling
- ➔ Debond Initiation
- ➔ Debond Propagation
- ➔ Conclusions



# INITIATION OF TRANSVERSE CRACKS IN THIN-PLIES

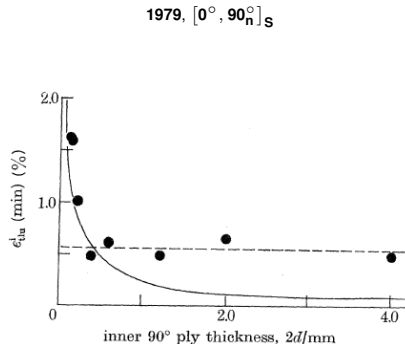
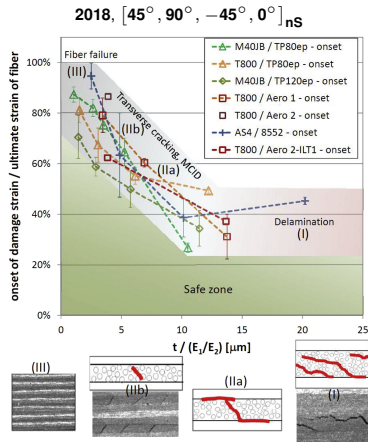
## The Thin-ply "Advantage": new material

2018,  $[45^\circ, 90^\circ, -45^\circ, 0^\circ]$  ns



Cugnoni et al., Compos. Sci. Technol. **168**, 2018.

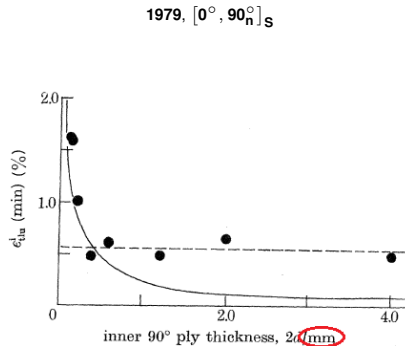
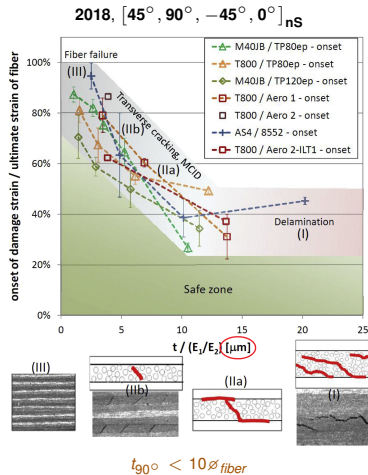
## The Thin-ply "Advantage": new material, old result



Cugnoni et al., Compos. Sci. Technol. **168**, 2018.

Bailey et al., P. Roy. Soc. A-Math. Phys. **366** (1727), 1979.

## The Thin-ply "Advantage": new material, old result?

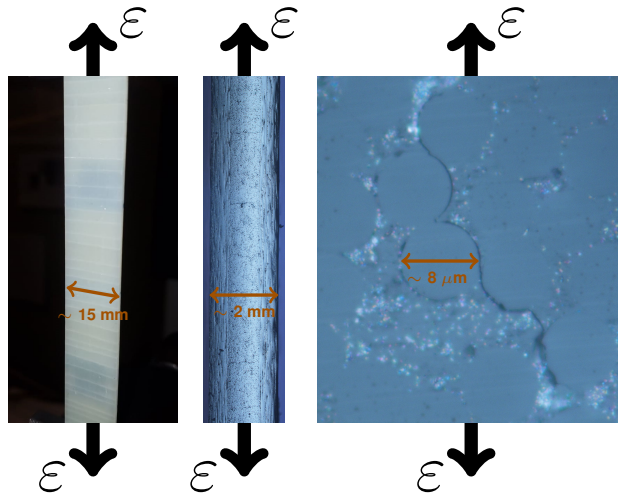


$t_{90^\circ} > 100\phi_{\text{fiber}}$

Cugnoni et al., Compos. Sci. Technol. **168**, 2018.

Bailey et al., P. Roy. Soc. A-Math. Phys. **366** (1727), 1979.

## Micromechanics of Initiation



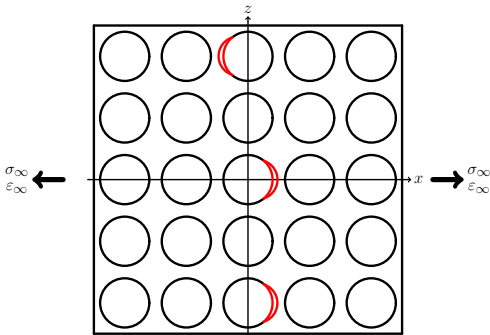
**Left:**  
front view of  $[0, 90]_S$ ,  
visual inspection.

**Center:**  
edge view of  $[0, 90]_S$ ,  
optical microscope.

**Right:**  
edge view of  $[0, 90]_S$ ,  
optical microscope.

## Micromechanics of Initiation

### Stage 1: isolated debonds



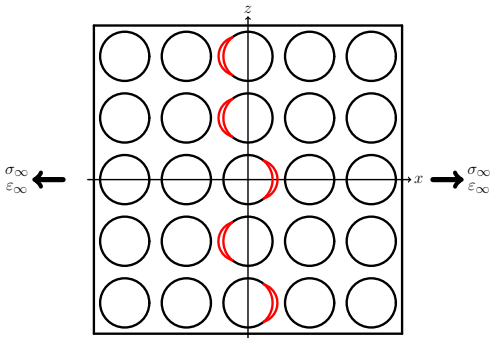
Bailey et al., P. Roy. Soc. A-Math. Phy. **366** (1727), 1979.

Bailey et al., J. Mater. Sci. **16** (3), 1981.

Zhang et al., Compos. Part A-Appl. S. **28** (4), 1997.

## Micromechanics of Initiation

### Stage 2: consecutive debonds



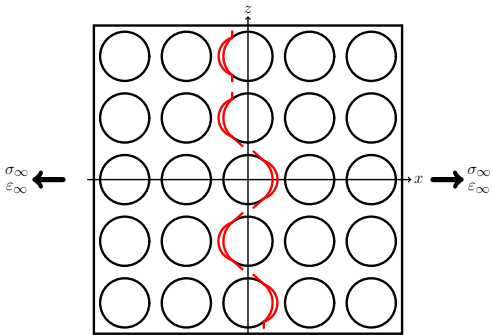
Bailey et al., P. Roy. Soc. A-Math. Phy. **366** (1727), 1979.

Bailey et al., J. Mater. Sci. **16** (3), 1981.

Zhang et al., Compos. Part A-Appl. S. **28** (4), 1997.

## Micromechanics of Initiation

### Stage 3: kinking



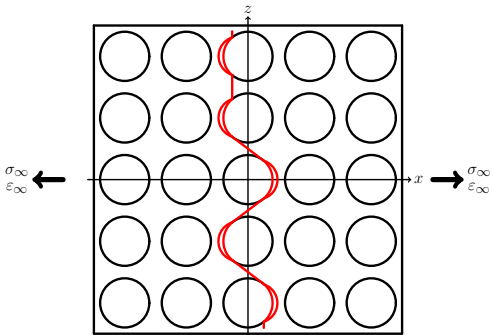
Bailey et al., P. Roy. Soc. A-Math. Phy. **366** (1727), 1979.

Bailey et al., J. Mater. Sci. **16** (3), 1981.

Zhang et al., Compos. Part A-Appl. S. **28** (4), 1997.

## Micromechanics of Initiation

### Stage 4: coalescence

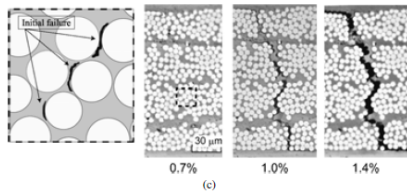


Bailey et al., P. Roy. Soc. A-Math. Phy. **366** (1727), 1979.

Bailey et al., J. Mater. Sci. **16** (3), 1981.

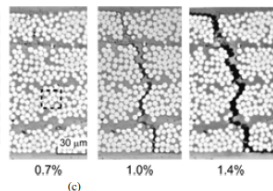
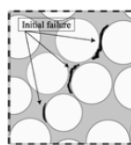
Zhang et al., Compos. Part A-Appl. S. **28** (4), 1997.

## A Counter-intuitive Observation

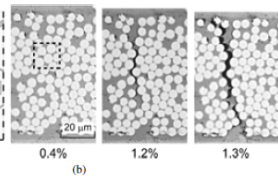
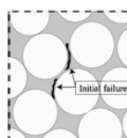
 $[0^\circ, 90_n^\circ]_S$ 

$$n = 4, t_{90^\circ} = 160 \mu m$$

## A Counter-intuitive Observation

 $[0^\circ, 90_n^\circ]_S$ 

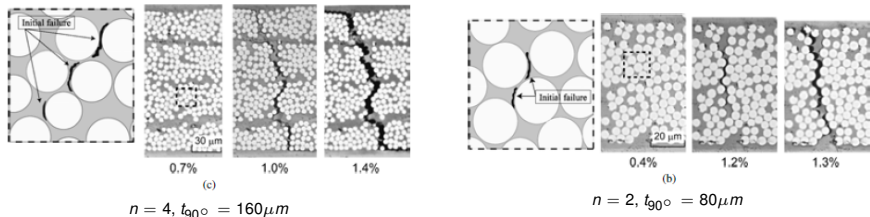
$$n = 4, t_{90^\circ} = 160 \mu m$$



$$n = 2, t_{90^\circ} = 80 \mu m$$

## A Counter-intuitive Observation

$[0^\circ, 90^\circ]_S$

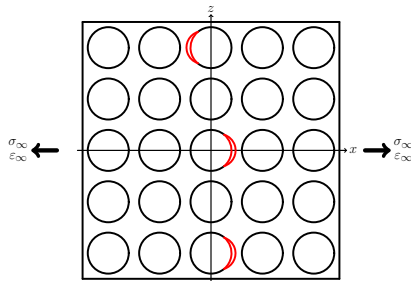


Saito et al., Adv. Compos. Mater. 21 (1), 2012.

## Objective of the Study

Can we talk about a ply-thickness effect for the fiber-matrix interface crack?

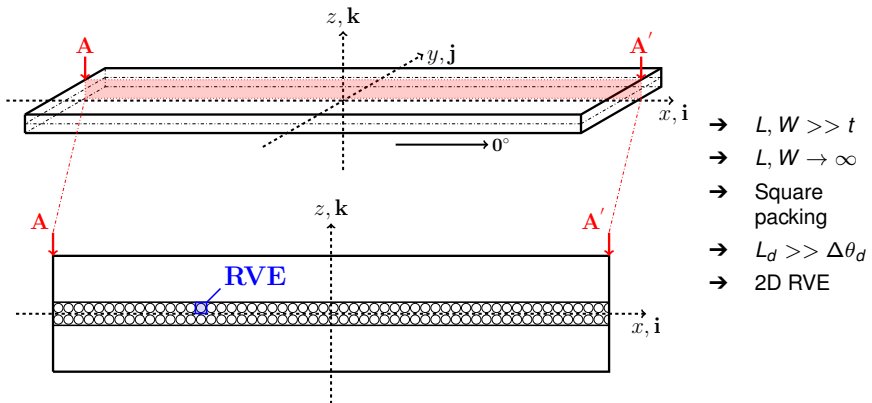
### Stage 1: isolated debonds



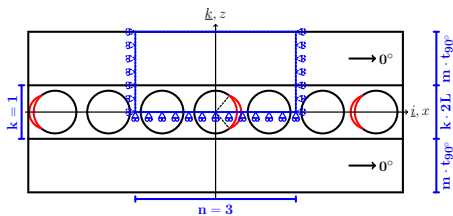
Initiation of Transverse Cracks in Thin-plies   Modeling   Debond Initiation   Debond Propagation   Conclusions  
Geometry   Representative Volume Elements   Assumptions   Solution

## MODELING

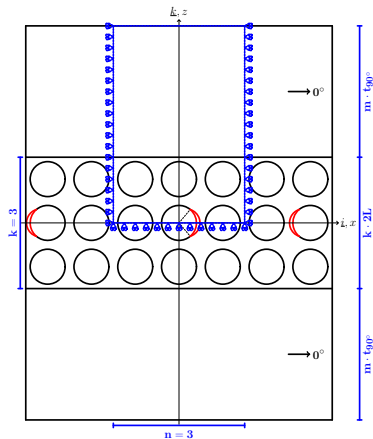
## Geometry



## Representative Volume Elements

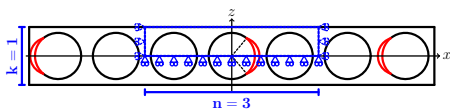


$$n \times 1 - m \cdot t_{90^\circ}$$



$$n \times k - m \cdot t_{90^\circ}$$

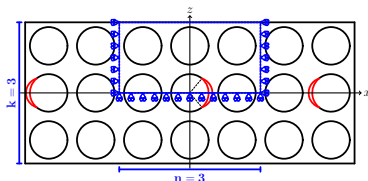
## Representative Volume Elements



– free

$n \times 1$  – coupling

– coupling +  $H$

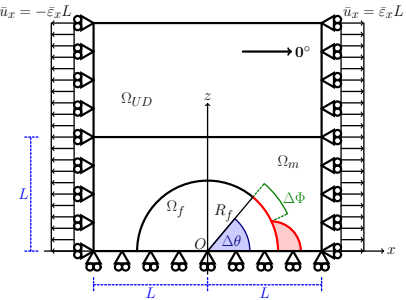


– free

$n \times k$  – coupling

– coupling +  $H$

## Assumptions

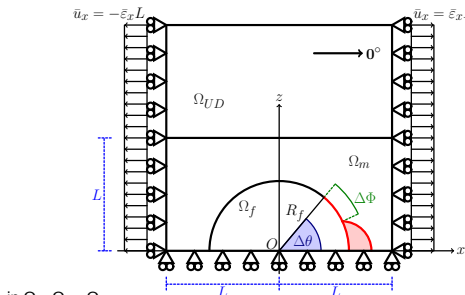


- Linear elastic, homogeneous materials
- Concentric Cylinders Assembly with Self-Consistent Shear Model for UD
- Plane strain
- Frictionless contact interaction
- Symmetric w.r.t. x-axis
- Coupling of x-displacements on left and right side (repeating unit cell)
- Applied uniaxial tensile strain epsilon\_x = 1%
- V\_f = 60%

$$R_f = 1 \text{ } [\mu\text{m}] \quad L = \frac{R_f}{2} \sqrt{\frac{\pi}{V_f}}$$

Material	$V_f$ [%]	$E_L$ [GPa]	$E_T$ [GPa]	$\mu_{LT}$ [GPa]	$\nu_{LT}$ [-]	$\nu_{TT}$ [-]
Glass fiber	-	70.0	70.0	29.2	0.2	0.2
Epoxy	-	3.5	3.5	1.25	0.4	0.4
UD	60.0	43.442	13.714	4.315	0.273	0.465

## Solution



in  $\Omega_f, \Omega_m, \Omega_{UD}$ :

$$\frac{\partial^2 \varepsilon_{xx}}{\partial x^2} + \frac{\partial^2 \varepsilon_{zz}}{\partial z^2} = \frac{\partial^2 \gamma_{zx}}{\partial x \partial z} \quad \text{for } 0^\circ \leq \alpha \leq \Delta\theta : \\ (\vec{r}_x(P_x, \alpha), \vec{r}_z(P_z, \alpha)) \cdot \vec{r}_x > 0$$

$$\varepsilon_V = \gamma_{xy} = \gamma_{yz} = 0$$

$$\frac{\partial \sigma_{xx}}{\partial t} + \frac{\partial \tau_{zx}}{\partial x} = 0 \quad \text{at } \Delta v \leq \alpha \leq 100 \text{ m/s}$$

$$\sigma_{ii} = E_{ijkl}\varepsilon_k$$

$$\frac{\partial \sigma_{zx}}{\partial x} + \frac{\partial \sigma_{zz}}{\partial z} = 0$$

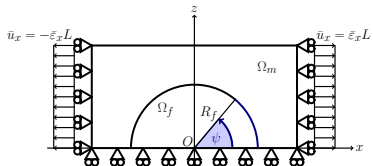
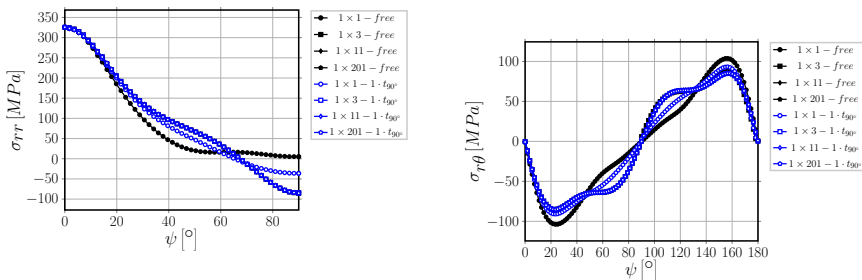
$$\sigma_{yy} = \nu (\sigma_{xx} + \sigma_{zz})$$

- oscillating singularity
 
$$\sigma \sim r^{-\frac{1}{2}} \sin(\varepsilon \log r), \quad V_f \rightarrow 0$$

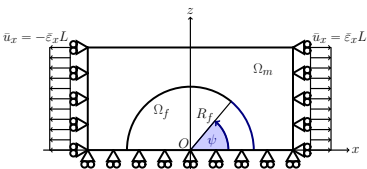
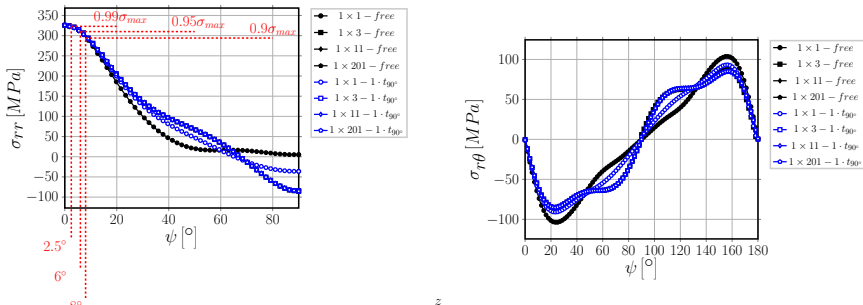
$$\varepsilon = \frac{1}{2\pi} \log \left( \frac{1-\beta}{1+\beta} \right)$$

$$\beta = \frac{\mu_2(\kappa_1 - 1) - \mu_1(\kappa_2 - 1)}{\mu_2(\kappa_1 + 1) + \mu_1(\kappa_2 + 1)}$$
  - receding contact
  - $\frac{G(R_{f,2})}{G(R_{f,1})} = \frac{R_{f,2}}{R_{f,1}}, \quad \frac{G(\bar{\varepsilon}_{x,2})}{G(\bar{\varepsilon}_{x,1})} = \frac{\bar{\varepsilon}_{x,2}^2}{\bar{\varepsilon}_{x,1}^2}$
  - FEM + LEFM (VCCT)
  - 2<sup>nd</sup> order shape functions
  - regular mesh of quadrilaterals at the crack tip:
    - $AR \sim 1, \quad \delta = 0.05^\circ$

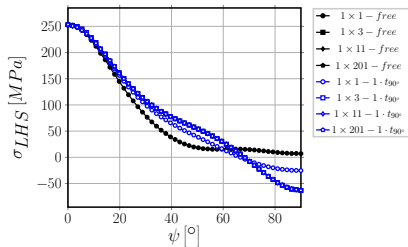
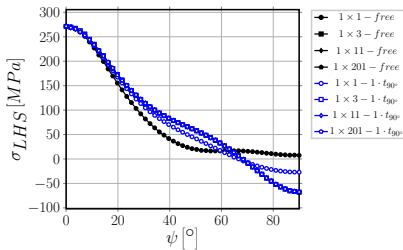
## DEBOND INITIATION

**$\sigma_{rr}$  vs  $\tau_{r\theta}$ : radial stress vs tangential shear at the interface**

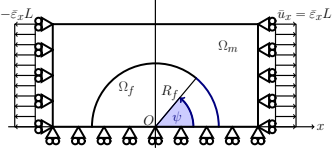
## $\sigma_{rr}$ vs $\tau_{r\theta}$ : radial stress vs tangential shear at the interface



## $\sigma_{LHS}$ : local hydrostatic stress at the interface

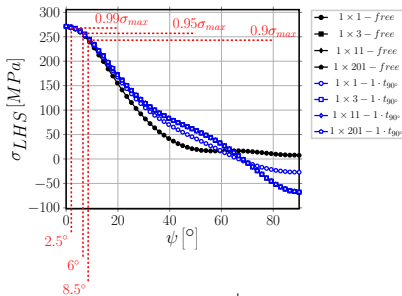


$$\sigma_{LHS}^{2D} = \frac{\sigma_{rr} + \sigma_{\theta\theta}}{2}$$

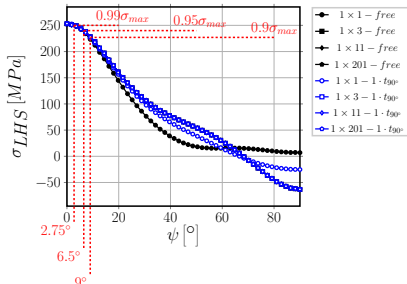
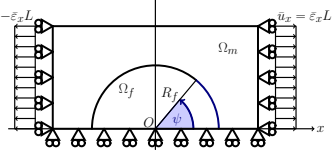


$$\sigma_{LHS}^{3D} = \frac{\sigma_{rr} + \sigma_{\theta\theta} + \sigma_{yy}}{3}$$

## $\sigma_{LHS}$ : local hydrostatic stress at the interface

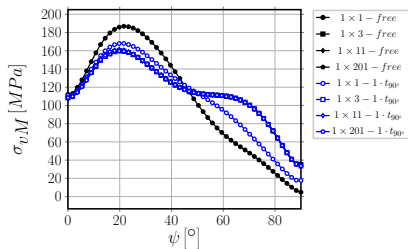
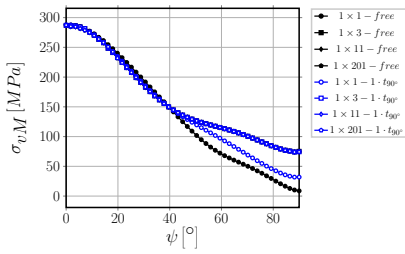


$$\sigma_{LHS}^{2D} = \frac{\sigma_{rr} + \sigma_{\theta\theta}}{2}$$



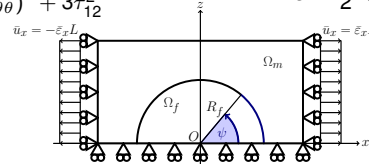
$$\sigma_{LHS}^{3D} = \frac{\sigma_{rr} + \sigma_{\theta\theta} + \sigma_{yy}}{3}$$

## $\sigma_{vM}$ : von Mises stress at the interface

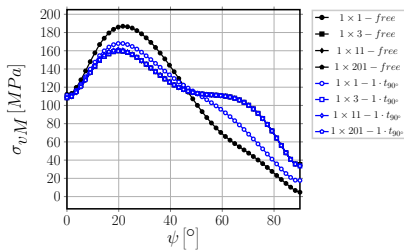
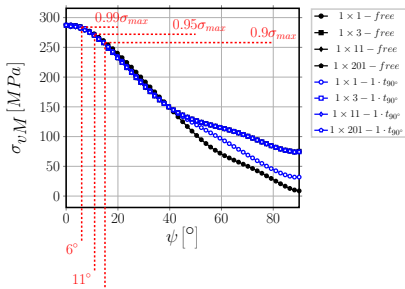


$$\sigma_{vM}^{2D} = \sqrt{(\sigma_{rr} - \sigma_{\theta\theta})^2 + 3\tau_{12}^2}$$

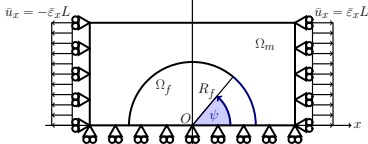
$$\sigma_{LHS}^{3D} = \frac{3}{2} s_{ij} s_{ij} \quad s_{ij} = \sigma_{ij} - \frac{1}{3} \sigma_{kk} \delta_{ij}$$



## $\sigma_{vM}$ : von Mises stress at the interface

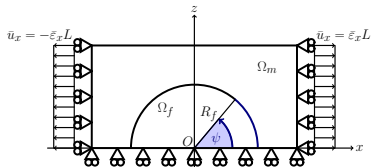
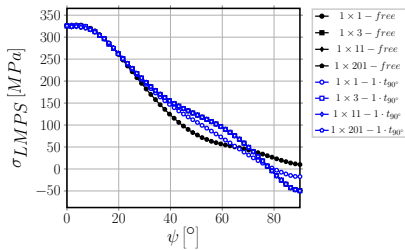
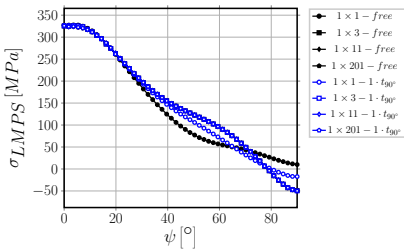


$$\sigma_{vM}^{2D} = \sqrt{(\sigma_{rr} - \sigma_{\theta\theta})^2 + 3\tau_{12}^2}$$

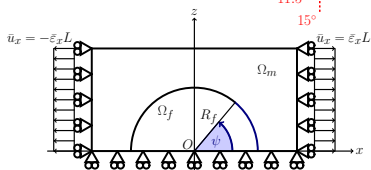
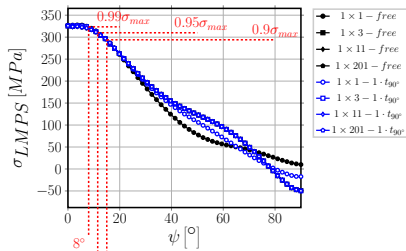
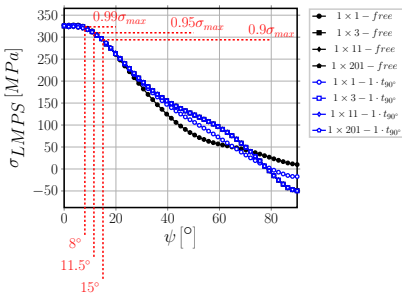


$$\sigma_{LHS}^{3D} = \frac{3}{2} s_{ij} s_{ij} \quad s_{ij} = \sigma_{ij} - \frac{1}{3} \sigma_{kk} \delta_{ij}$$

## $\sigma_I$ : maximum principal stress at the interface



## $\sigma_I$ : maximum principal stress at the interface



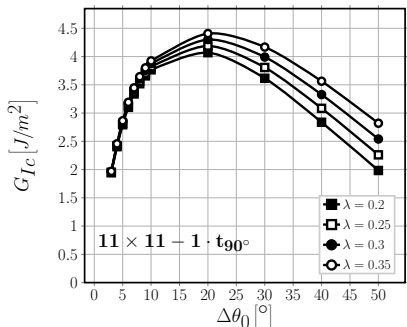
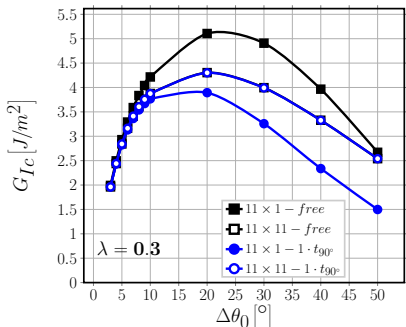
## Summary



Initiation of Transverse Cracks in Thin-plies   Modeling   Debond Initiation   Debond Propagation   Conclusions  
Estimation of  $G_{lc}$    Estimation of  $\Delta\theta_{max}$

## **DEBOND PROPAGATION**

## Estimation of $G_{Ic}$

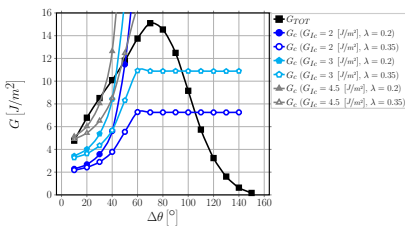


$$G_{Ic} = \frac{G_c}{1 + \tan^2((1 - \lambda) \Psi_G)} \Big|_{G_c=G_{TOT}(\Delta\theta_0)},$$

$$\Psi_G = \tan^{-1} \left( \sqrt{\frac{G_{II}}{G_I}} \right) \Big|_{\Delta\theta_0}$$

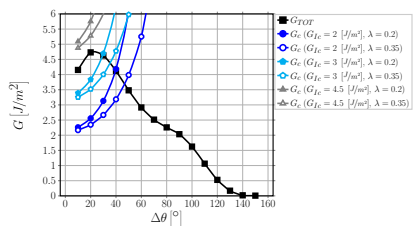
## Estimation of $\Delta\theta_{max}$

$21 \times 1 - free$



$$\Delta\theta_{max} \in (30^\circ - 105^\circ)$$

$21 \times 1 - 1 \cdot t_{90^\circ}$

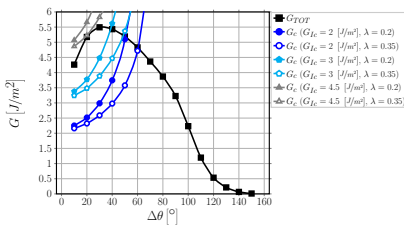


$$\Delta\theta_{max} \in (30^\circ - 50^\circ)$$

$$G_{TOT}(\Delta\theta) > G_c = G_{lc} \left( 1 + \tan^2((1 - \lambda)\Psi_G) \right), \quad \Psi_G = \tan^{-1} \left( \sqrt{\frac{G_{II}}{G_I}} \right) \Big|_{\Delta\theta}$$

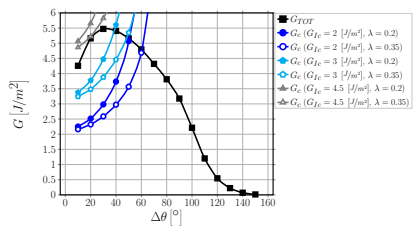
## Estimation of $\Delta\theta_{max}$

$21 \times 3 - free$



$$\Delta\theta_{max} \in (40^\circ - 60^\circ)$$

$21 \times 3 - t_{90^\circ}$

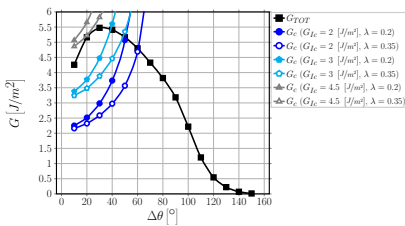


$$\Delta\theta_{max} \in (40^\circ - 60^\circ)$$

$$G_{TOT}(\Delta\theta) > G_c = G_{lc} \left( 1 + \tan^2((1-\lambda)\Psi_G) \right), \quad \Psi_G = \tan^{-1} \left( \sqrt{\frac{G_{II}}{G_I}} \right) \Big|_{\Delta\theta}$$

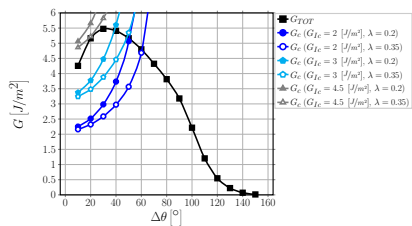
## Estimation of $\Delta\theta_{max}$

$21 \times 21 - free$



$$\Delta\theta_{max} \in (40^\circ - 60^\circ)$$

$21 \times 21 - 1 \cdot t_{90^\circ}$

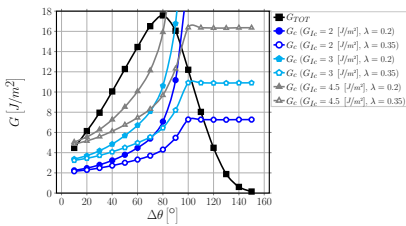


$$\Delta\theta_{max} \in (40^\circ - 60^\circ)$$

$$G_{TOT}(\Delta\theta) > G_c = G_{lc} \left( 1 + \tan^2((1-\lambda)\Psi_G) \right), \quad \Psi_G = \tan^{-1} \left( \sqrt{\frac{G_{II}}{G_I}} \right) \Big|_{\Delta\theta}$$

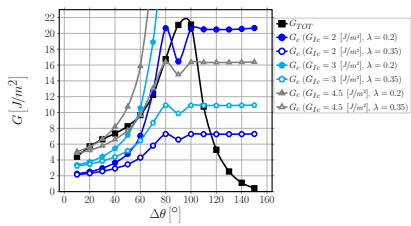
## Estimation of $\Delta\theta_{max}$

$21 \times 21 - symm$



$$\Delta\theta_{max} \in (80^\circ - 110^\circ)$$

$21 \times 21 - asymm$



$$\Delta\theta_{max} \in (55^\circ - 115^\circ)$$

$$G_{TOT}(\Delta\theta) > G_c = G_{lc} \left( 1 + \tan^2((1 - \lambda) \Psi_G) \right), \quad \Psi_G = \tan^{-1} \left( \sqrt{\frac{G_{II}}{G_I}} \right) \Big|_{\Delta\theta}$$

## CONCLUSIONS

## Conclusions

- No effect of  $90^\circ$  ply thickness can be observed when  $t_{90^\circ}$  is at least  $\sim 3\phi_{fiber}$
- Only if  $t_{90^\circ}$  is reduced to  $1\phi_{fiber}$ , ERR is reduced for a given level of applied strain, i.e. debond growth is delayed to higher levels of applied strain ( $G \sim \varepsilon_{applied}^2$ )
- No effect of  $0^\circ$  ply thickness can be observed when  $t_{0^\circ}/t_{90^\circ} > 1$
- A small difference can be observed when  $t_{0^\circ} = t_{90^\circ}$ , due to the smaller bending stiffness of a thinner  $0^\circ$  layer



LULEÅ  
UNIVERSITY  
OF TECHNOLOGY



Education and Culture

Erasmus Mundus